



FAILURE ANALYSIS OF A BASE SUPPORT PLATE OF A SEMOLINA PURIFIER MACHINES SUBJECTED TO FATIGUE LOADING

¹Yunus DERE , ^{2*}Hakkı EKEM , ³Ömer Sinan ŞAHİN , ⁴Hasan Hüsnü KORKMAZ 

¹Necmettin Erbakan University, Engineering Faculty, Civil Engineering Department, Konya, TÜRKİYE

²IMAS Integrated Machines Co. Research and Development Center, Konya, TÜRKİYE

³Konya Technical University, Engineering and Natural Sciences Faculty, Mechanical Engineering Department,
Konya, TÜRKİYE

¹ydere@erbakan.edu.tr, ²hakki.ekem@imas.com.tr, ³ossahin@ktun.edu.tr,

⁴hasanhusnukorkmaz@gmail.com

Highlights

- The design of the semolina purifier machine, which is frequently used in the milling industry and is subject to fatigue, was examined.
- Finite element method was used in design improvements.
- Similarly, approaches that will be essential in the design of machines subject to fatigue have been tried to be put forward.



FAILURE ANALYSIS OF A BASE SUPPORT PLATE OF A SEMOLINA PURIFIER MACHINES SUBJECTED TO FATIGUE LOADING

¹Yunus DERE , ^{2*}Hakkı EKEM , ³Ömer Sinan ŞAHİN , ⁴Hasan Hüsnü KORKMAZ 

¹Necmettin Erbakan University, Engineering Faculty, Civil Engineering Department, Konya, TÜRKİYE

²IMAS Integrated Machines Co. Research and Development Center, Konya, TÜRKİYE

³Konya Technical University, Engineering and Natural Sciences Faculty, Mechanical Engineering Department,
Konya, TÜRKİYE

¹ydere@erbakan.edu.tr, ²hakki.ekem@imas.com.tr, ³ossahin@ktun.edu.tr,

⁴hasanhusnukorkmaz@gmail.com

(Received: 13.09.2023; Accepted in Revised Form: 12.12.2023)

ABSTRACT: The semolina purifier is a machine used in the production phase in flour factories and is exposed to fatigue loads. In this study, the reason for the damage when a semolina purifier machine breaks during use and the improvements that need to be made in the design are discussed. For this purpose, a finite element model (FEM) was created using ABAQUS software. As a result of the analysis, it was determined that the design of the machine support platform should be improved. A two-stage strengthening alternative is designed. The cyclic loads applied by the twin motors that move the machine screens are applied in the FEM model. The deformations and stresses occurring in the reinforced and existing design machine base plate were compared. The results showed that, the maximum equivalent stress level can be reduced from 86 MPa to 35 MPa by design improvements made on the base plate.

Keywords: Failure, Fatigue, Semolina purifier machine, Strengthening

1. INTRODUCTION

Maintenance of critical equipment to ensure high levels of reliability, availability, and performance is one of the major concerns on today's industrial sector especially for rotation machines [1-4] and other conventional type machines [5-8] subjected to cyclic loading. Unexpected failures can lead to substantial losses, either from the maintenance procedure itself or from the resulting production halts [9-12]. In order to proactively prevent failure of components, failure modes in functional component's caused by the damage/fracture modes of the materials should be comprehensively determined. Failure analysis is a process performed in order to determine the root causes or factors that led to an undesired loss of functionality. The immediate objective is to find the root causes of the failure in order to obtain the compensation for the induced damage even if the really important is to prevent similar failures in new components [3]. Literature review revealed that fatigue and Failure analysis of various machines and machine parts such as anti-return valve of a high pressure machine [13], yarn twisting machine [14], diesel engine injector [15], excavator buckets [16], welded steel plates for conveyor belts [17], aluminum alloy elastic coupling [18], friction-stir welded joints [19, 24], bridge conveyor [20], cutting blades [21] and gear and transmission shafts [22, 23]. The subject of fatigue damage development and design according to fatigue damage is a subject that has been studied extensively in the literature. However, there are no studies on fatigue damage and fatigue-based design in special purpose machines such as semolina purification machines. This study will fill this gap.

Semolina is a type of flour made only from durum wheat. It is obtained by grinding and sieving durum wheat. In English, semolina is an extract from the word "coarsely ground wheat flour. The term semolina is also used to designate coarse middlings from other varieties of wheat. It is expressed by the words "semola" in Italian, "simil" in Latin and "semidalis" in ancient Greek. Semolina is divided into 5 groups according to its grain size (Figure 1). Semolina between 125-300 microns is used for pasta production and 1120 microns and above is "whole wheat" semolina. Semolina is yellow in color, bright and angular.

*Corresponding Author: Hakkı EKEM, hakki.ekem@imas.com.tr



Figure 1. Types of semolina

Durum wheat is grown mainly in the Middle East and accounts for about 5-8% of the world's cultivated wheat amount. Semolina contains 73% carbohydrates. There is approximately 360 kcal of energy in 100 grams of semolina.

Semolina contains high amount of gluten and for this reason it is preferred to make pasta. The semolina helps to maintain the shape of the pasta during cooking. The main difference between semolina and flour is that semolina can be a better coarse and darker shade and more yellow than traditional flour. It is important to carefully clean and grind the wheat to prevent the presence of stains in the semolina. Semolina quality directly affects the pasta quality.

Semolina purifiers are machines used in flour and semolina factories to purify, classify and clean semolina from crushing rolls and lyso rolls. (Figure 2). The purifier consists of four main parts (Figure 3):

- A fixed main frame
- Oscillating body containing sieves
- One suction channel
- Exhaust chamber,

The machine is produced as a monolithic moving body with two vibro motors and a three-layer sieve system. The three sieve layers are angled according to the ground. These sieves oscillate on the fixed main chassis. The oscillation of the sieves is provided by two eccentric motors at the end of the machine (Figure 3). The product coming from the inlet is evenly distributed on the sieve surface with the adjustable valves and the vibration effect of the machine. In three-row boxes, the desired amount and type of product is obtained according to its shape.



Figure 2. Semolina purifier machine

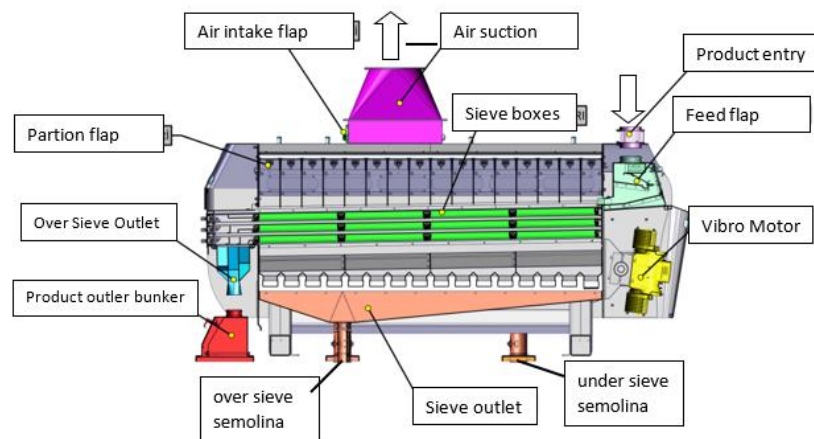


Figure 3. Main components of purifier machine

The product enters the machine from the top in a way that the flow rate can be adjusted. It should be homogeneously distributed over the whole screen surface. The purifier provides mobility to the semolina by moving the tray with the sieves thanks to its vibration motor. The motors that make an upward angle with the horizontal make the particles an inclined projection motion (Figure 4). Thus, the surface of the products is expanded. Air, which enters from the bottom of the sieves and goes upwards, creates a vacuum effect. The particles, whose adhesion surface is expanded, are separated and pushed to the outlet channel by keeping them suspended with vacuum. It is then moved to the collection box below. Due to more than one sieve, the product can be separated according to the particle size. The air entering the machine leaves the machine from the top by passing through the air ducts after passing through the sieves (Figure 5).

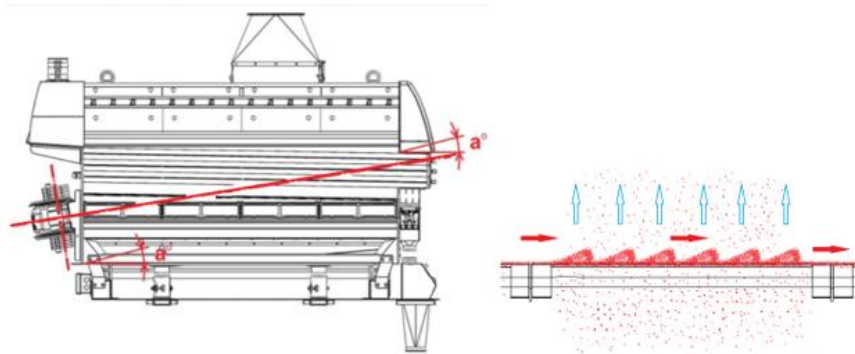


Figure 4. Inclined projection of particles in purifier machine

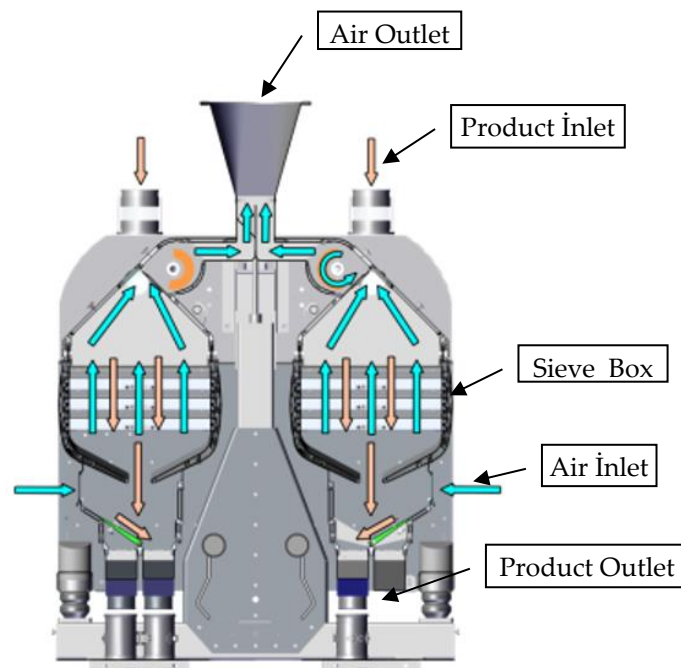


Figure 5. Air flow chart in purifier machine

2. MATERIAL AND METHODS

The design of the traditional semolina purifier machine, which is exposed to variable loads, is examined. The fracture surface examined by optical microscopy and evaluation revealed that the base plates fractured under fatigue failure.

As a result of the examination, it was determined that the design of the machine support platform should be improved and two different reinforcement alternatives were designed. The conventional design and new design alternatives were modelled by using ABAQUS finite elements software. The strengthened and current design is compared through the deformations and stresses occurring in the machine base plate.

The cyclic loads applied by the twin motors that move the machine screens are applied in the FEM model. The deformations and stresses occurring in the reinforced and existing design machine base plate were compared. The analysis-review and update procedure is conducted in accordance with methodology shown in Figure 6.

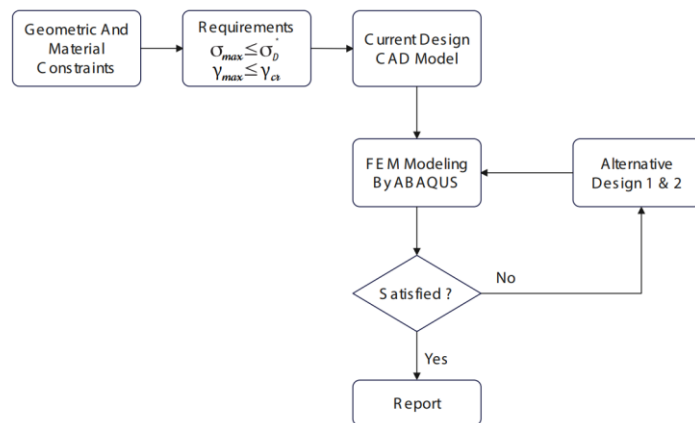


Figure 6. Flowchart of the analysis procedure

A three-dimensional finite element model of the machine was created in order to investigate the cause of the fatigue failure in the sub-frame of the purifier machine and to evaluate the strengthening alternatives. Numerical study was carried out in the ABAQUS software (Figure 10). Mechanical properties of materials used in analysis is given in Table 1.

Table 1. Mechanical properties of machine components

Material	Young Modulus (GPa)	Poisson's ratio	Density (kg/m ³)
AISI-430	200	0.28	7850
AL-5083	71	0.33	2650
AL-6061	69	0.33	2690
C-1010	200	0.28	7850
ST-37	200	0.3	7850
ST-42	200	0.3	7850

The elastomeric bearings on the machine base are modeled as springs in the FE model. Spring constants were supplied by the manufacturer of the elastomeric bearings. For the vertical and lateral movement, different values are defined. The vertical spring constant was defined as 328 N/mm and the lateral spring constant was defined as 340 N/mm.

3. RESULTS AND DISCUSSIONS

3.1. Description of Fracture Failure

In the semolina purifier, the moving body is obtained with two vibro motors (Figure 8). The movable sieve part is placed on the fixed chassis. The fixed chassis is placed on four elastomeric supports. The chassis rests on two 20 mm thick plates (Figure 9).

These are the machines produced and sold by the manufacturer company. Breakage problems in the support plates have been reported after prolonged use of the machines. Said plates are shown in green in Figure 8. Fracture occurred at the corners where the plates were attached to the elastomeric support (Figure 9). The manufacturer contacted the authors to determine the cause of the damage to the support sheet of the machine and to determine the strengthening methods. It is desired that the retrofit to be developed can also be applied to machines that have been sold before and are still in use.

is examined, it is seen that the displacement value of the support leg in the $-Z$ direction is 2.08 mm. Here the relative displacement was obtained as 5.35 mm. The von Mises equivalent stress distribution on the support plate is given in Figure 12-a. As seen in this figure, the maximum equivalent stress was obtained as 35 MPa.

In the second stage of the study, in addition to the machine weight, the sinusoidal variable force created by the twin vibromotors on the side of the machine was applied to the model. The time-dependent variation of periodic loading is shown in Figure 13. There are rubber vibration damping elements at four points where the machine chassis is connected to the ground. The mechanical properties of these components are defined in the software. The distribution of horizontal displacements obtained under dynamic loading on the support plate is given in Figure 14-a. Here the relative displacement was obtained as 23.4 mm. The von Mises stress distribution obtained in the support plate under dynamic loads is given in Figure 15-a. As seen in this figure, the maximum equivalent stress was obtained as 86 MPa.

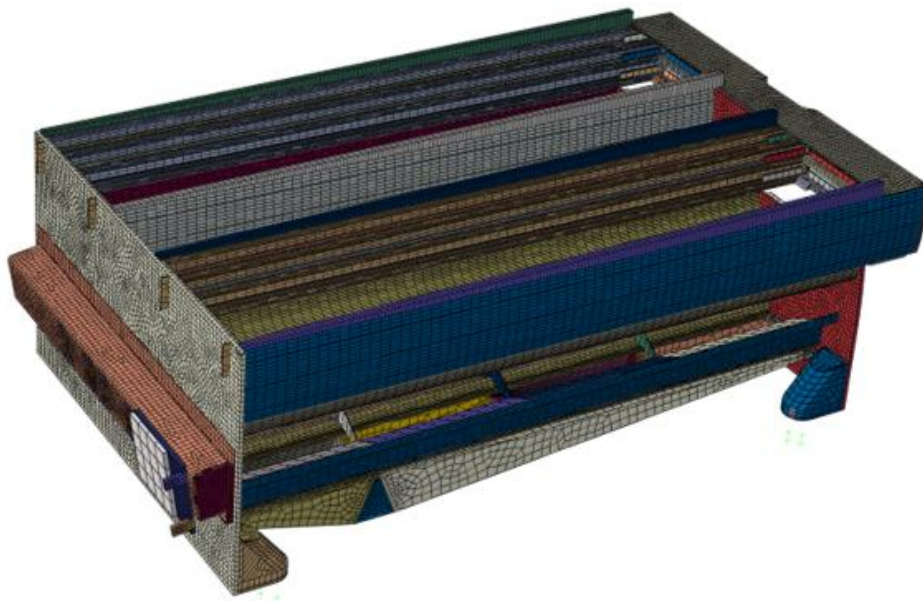


Figure 10. Finite element model of purifier machine

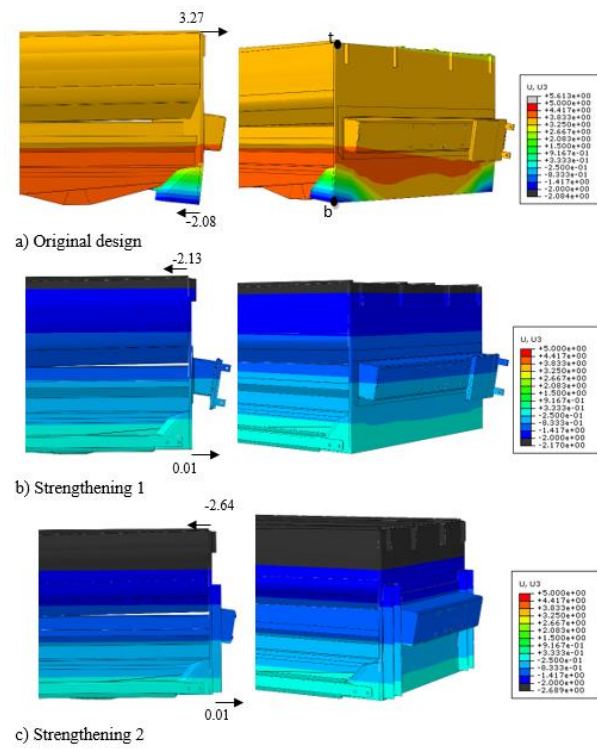


Figure 11. Lateral displacement distribution of purifier machine under self-weights (mm)

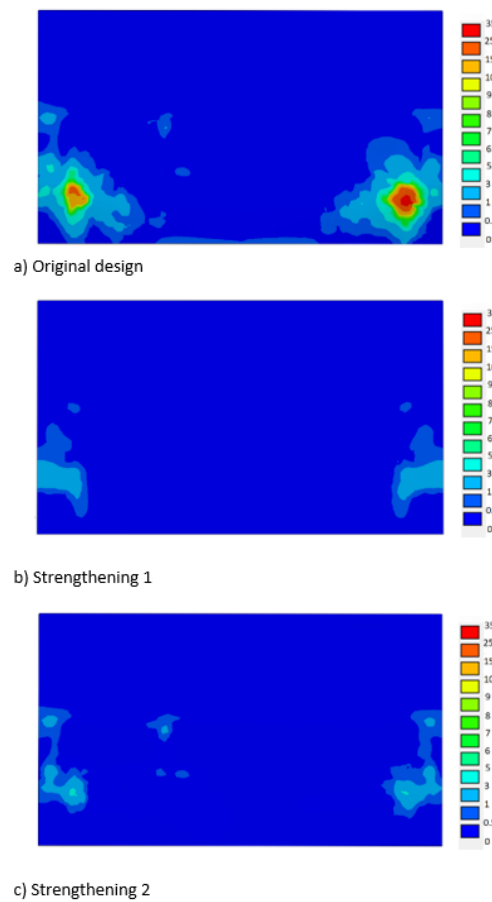


Figure 12. Von Misses stress distribution of side support plate (motor side) (self-weight) (MPa)

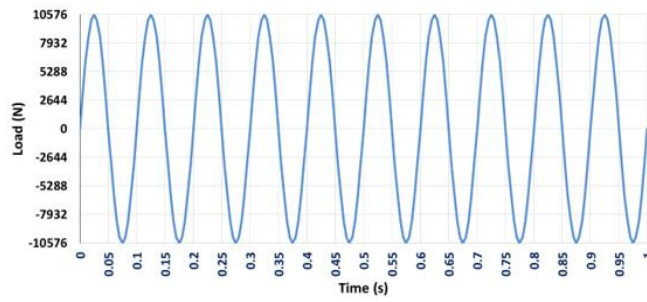


Figure 13. Cyclic loading of twin motors

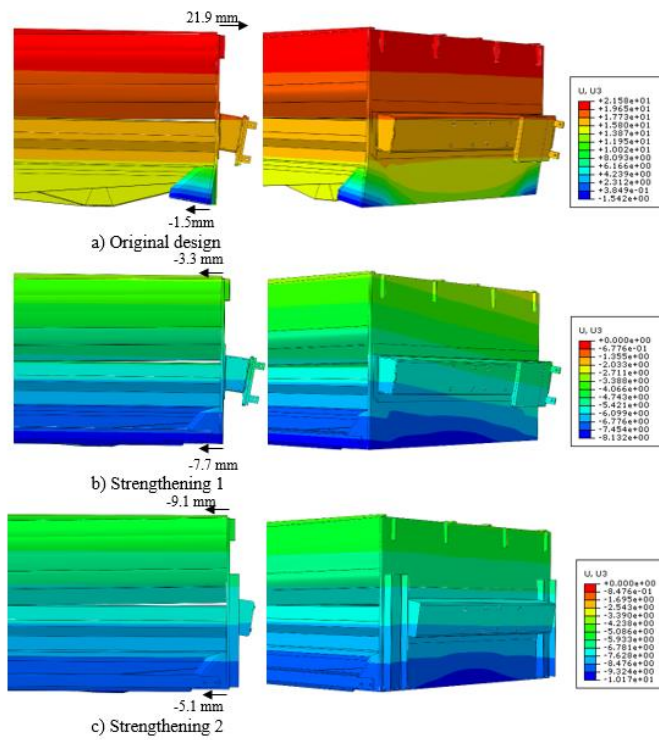


Figure 14. Lateral displacement distribution of support plate region under dynamic loading (mm)

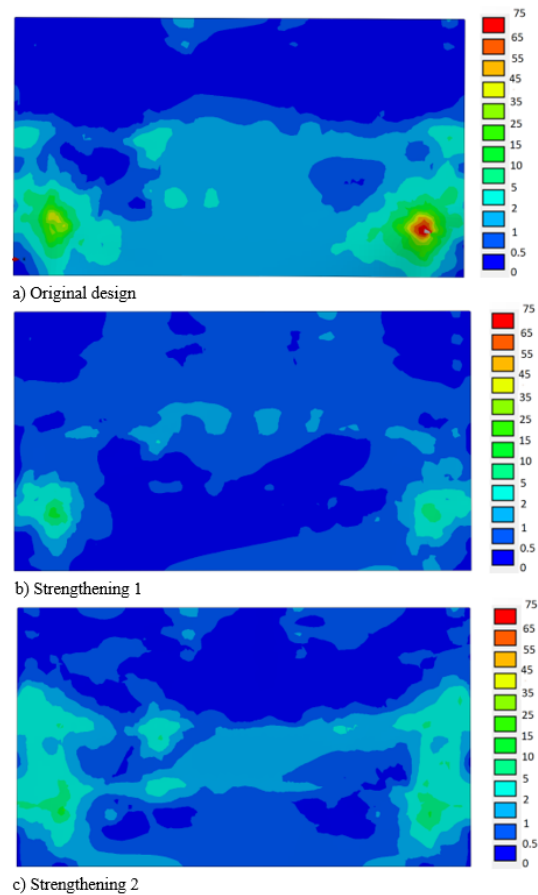


Figure 15. Von Misses stress distribution of side support plate (motor side) (MPa) (cyclic loading)

3.3. Retrofit Alternatives and FEM Results

When the fatigue damages observed on the motor plate (Figure 9) and the FEM analysis results were evaluated, it was concluded that the motor support plate was insufficient against fatigue loads. So, it was concluded that a design improvement is needed to eliminate this negativity. However, the machine consists of many components and has complex connections. So, design improvements must not seriously affect the production and assembly process of the machine. In this context, two different reinforcement alternatives are planned.

In the first alternative, the lower support legs of the machine are connected to each other horizontally with 2 U-shaped steel elements (Figure 16). This alternative is called “First alternative strengthening”. The second alternative was called “First alternative strengthening”. Here, in addition to the steel elements mentioned in the first alternative, U-shaped reinforcement elements were mounted upwards from both sides of the support plate. (Figure 17). Later, reinforcement elements were included in the FEM model and the analyzes were repeated. Figure 11-b-c shows the lateral displacement distributions of reinforcement alternatives. Here, the relative displacements of the upper (“t”) and lower (“b”) points of the support plate were also obtained. Table 2 shows the relative displacement values. Compared to the relative displacement of 5.35 mm in the original design, it was obtained 2.14 mm displacement in the first strengthening alternative and 2.64 mm in the second alternative.

Table 2. Relative displacements of the models

		Displacement (mm)	Decrease (%)
Self-Weight	Current Design	5.35	-
	1 st Alternative Strengthening	2.14	-60
	2 nd Alternative Strengthening	2.65	-50.4
Dynamic Loading	Current Design	23.46	-
	1 st Alternative Strengthening	4.44	-81
	2 nd Alternative Strengthening	4.06	-82.7

In Figure 14-b and c, under cyclic dynamic loading, lateral displacement distributions for the 1st and 2nd strengthening alternatives are presented. The top and bottom points of the vibromotor side plate is marked as "t" and "b" in Figure 11-a. The relative displacement (Z direction) of the "t" and "b" points are calculated and given in Figure 18. Maximum relative displacement is calculated as 23.46 mm for original design, 4.44 mm for first strengthening alternative and 4.06 mm for second strengthening alternative. The relative displacements of the "t" and "b" points under cyclic loadings are given in Figure 18.

The bearing plate on the side where the twin vibromotors are connected has been examined. The obtained stresses, under the machine's dead weight (on the support plate) are given in Figure 12-a-c for original design, 1st strengthening alternative and 2nd strengthening alternative, respectively. A maximum stress of 6.24 MPa occurred in the 1st alternative application and a maximum of 3.7 MPa in the 2nd alternative application. Also, in Figure 15 a-b-c, corresponding stresses under dynamic loading are depicted.

The time dependent variation of the maximum equivalent stress formed under cyclic loading in the support plate is given in Figure 18. In this graph, the stress variation obtained from the original design and the models with strengthening alternatives is also given. The maximum values are tabulated in Table3.

Table 3. Maximum equivalent stress values

		Stress (MPa)	Decrease (%)
Self-Weight	Current Design	34	-
	1 st Alternative Strengthening	6.24	-81.6
	2 nd Alternative Strengthening	3.7	-89.1
Dynamic Loading	Current Design	86	-
	1 st Alternative Strengthening	20	-76,7
	2 nd Alternative Strengthening	15.4	-82.1

Considering the above listed design and analysis results, the production of the machine is revised, and the final design of the machine is shown in Figure 20.



Figure 16. First alternative strengthening steel rods connecting machine bottom legs

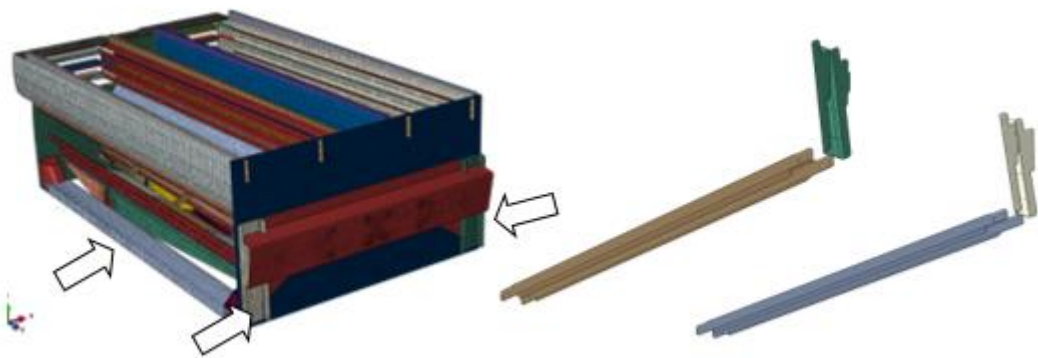


Figure 17. Second alternative strengthening

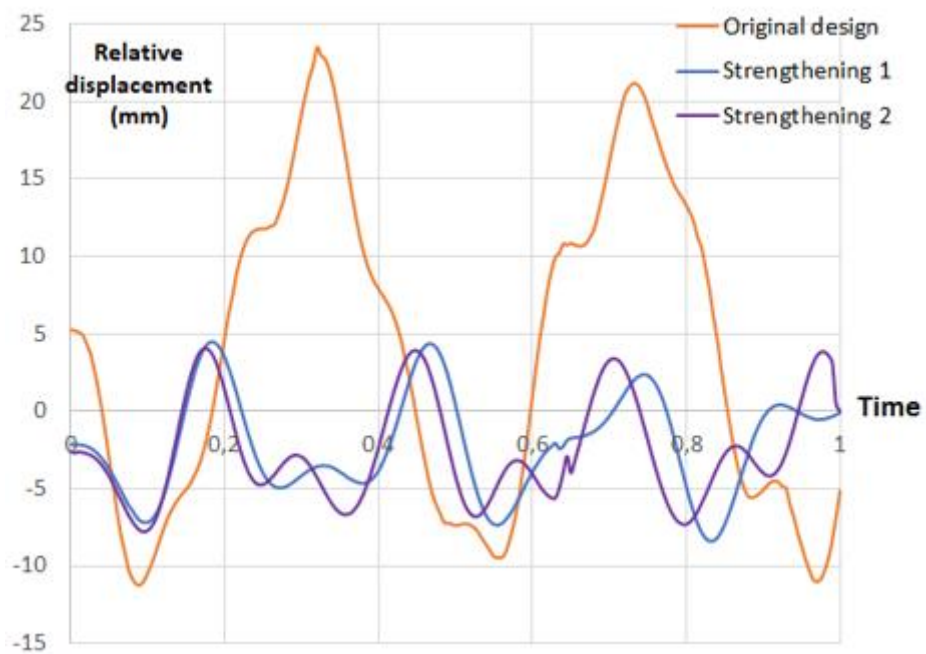


Figure 18. Relative displacement of side plate under cyclic loading

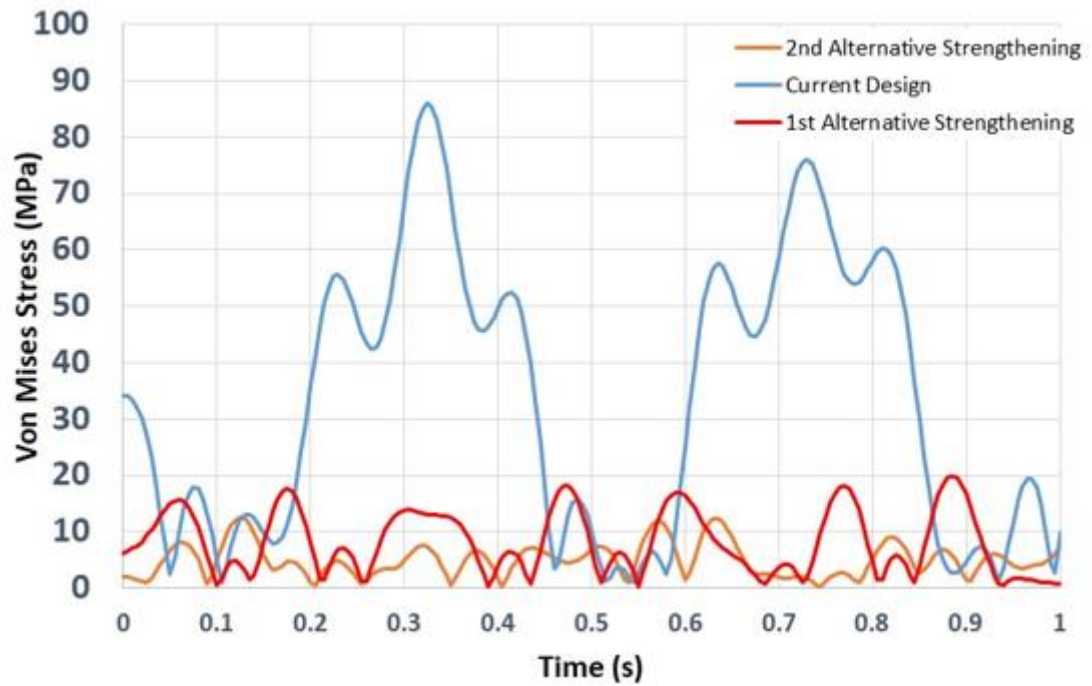


Figure 19. Maximum stress on bearing plates during cyclic loading



a) Rear view



b) Front view

Figure 20. Final design of the machine

4. CONCLUSIONS

It was concluded that the base support plates of the original design of the machine were insufficient for fatigue loading and susceptible to high cycle fatigue. Under cyclic loading, the initially displaced plate breaks under the effect of bending due to fatigue damage and the fatigue crack starts from one edge and proceeds to the other edge, passing through the nearest screw hole.

In this study, different strengthening alternatives have been proposed and analyzed in order to limit the deformations of the base support plates under static and dynamic loads and to prevent fatigue failure. The effectiveness of the proposed strengthening alternatives was evaluated according to the relative displacement of the upper and lower edges of the base support plate and the maximum Von Mises stresses occurring on the plate.

The 1st strengthening alternative decreased the relative displacement by -%60 for the self-weight case and -%50,4 for the dynamic case while the 2nd strengthening alternative decreased the relative displacement by -%81 for the self-weight case and -%82.7 for the dynamic case. On the other hand, the 1st

strengthening alternative decreased the maximum stress by -%81.6 for the self-weight case and -%89.1 for the dynamic case. The 2nd strengthening alternative decreased the maximum stress -%76,7 for the self-weight case and -%82,1 for the dynamic case. It is concluded that, reducing the stress and strain levels about %70 can result in considerable increase in fatigue life of constituents made of aluminum.

It is concluded that the stresses formed in the support plates after the strengthening remain well below the elastic limits. Static and dynamic analysis of computer models of the strengthening alternatives showed that the 2nd strengthening alternative was more effective in reducing the relative displacements between the edges of the support plate and the maximum Von Mises stresses. Therefore, alternative 2 was adopted as a preventative solution to a possible breakage failure in the support plate. Retrofit can be applied to existing treatment machines without too many changes to the structural system. It is also an economical solution as it requires additional steel elements that can be easily produced and shipped to worldwide demanded locations.

Acknowledgement

We would like to thank to the Imas Machinery Co. (Konya/TURKEY) for supporting the current work.

Conflict of Interest

Authors declare no conflicts of interest.

Author Contributions

Author contributions are as follows:

- 1st Author FEM Modelling and evaluation
- 2nd Author FEM Modelling and evaluation
- 3rd Author: Performing design studies, manuscript preparation
- 4th Author: FEM results evaluation, manuscript preparation

REFERENCES

- [1] M. A. Marins, F. M. L. Ribeiro, S. L. Netto, and E. A. B. Silva, "Improved similarity-based modeling for the classification of rotating-machine failures," *Journal of the Franklin Institute*, vol. 355, ss. 1913–1930, 2018.
- [2] T. Okabea and Y. Otsuka, "Proposal of a Validation Method of Failure Mode Analyses based on the Stress-Strength Model with a Support Vector Machine," *Reliability Engineering and System Safety*, vol. 205, 2021.
- [3] A. M. Irisarri, and E. Silveira, "Study of the failure of one machining tool," *Engineering Failure Analysis*, vol. 17, pp. 380–386, 2010.
- [4] F. Delgado, J. J. Coronado, and S. A. Rodríguez, "Failure analysis of a machine support for fique fibre processing," *Engineering Failure Analysis*, vol. 56, pp. 58-68, 2015.
- [5] X. Zhao, W. Ke, S. Zhang, and W. Zheng, "Potential failure cause analysis of tungsten carbide end mills for titanium alloy machining," *Engineering Failure Analysis*, vol. 66, pp. 321-327, 2016.
- [6] S. Papadopoulou, I. Pressas, A. Vazdirvanidis, and G. Pantazopoulos, "Fatigue failure analysis of roll steel pins from a chain assembly," *Engineering Failure Analysis*, vol. 101, pp. 320-328, 2019.
- [7] P. V. Krot, and R. Zimroz, "Failure analysis and modernization of high-pressure hydraulic press for drilling tubes testing," *Engineering Failure Analysis*, vol. 117, 2020.
- [8] Y. Li, P. Lu, B. Wang, Q. Xiang, and B. Ma, "Failure analysis of bolts on fatigue test bench for excavator stick," *Engineering Failure Analysis*, vol. 118, 2021.
- [9] T. Saraçyakupoglu, "Fracture and failure analysis of the trainer aircraft rudder pedal hanger,"

- Engineering Failure Analysis*, vol. 122, 2021.
- [10] M. Caliskan, "Evaluation of bonded and bolted repair techniques with finite element method," *Materials and Design*, vol. 27, pp. 811–820, 2006.
- [11] A. J. Wanga, Z. Guoa, X. Y. Jiaoa, L. Songc, W. X. Huc, J. C. Lic, and S. M. Xionga, "On the failure mechanism for high pressure die casting A390 hypereutectic alloy in low cycle and high cycle fatigue," *Materials Science and Engineering*, vol. 723, pp. 48-55, 2018.
- [12] C. Sasikumar, S. Srikanth, and S. K. Das "Analysis of premature failure of a tie bar in an injection molding machine," *Engineering Failure Analysis*, vol. 13, pp. 1246–1259. 2006.
- [13] J. M. Alegre, M. Preciado, and O. Ferren, "Study of the fatigue failure of an anti-return valve of a high pressure machine," *Engineering Failure Analysis*, vol. 14, pp. 408–416, 2007.
- [14] B. Tadic, P. M. Todorovic, Dj. Vukelic, and B. M. Jeremic, "Failure analysis and effects of redesign of a polypropylene yarn twisting machine," *Engineering Failure Analysis*, vol. 18, pp. 1308-1321, 2011.
- [15] X. Xu, Z. Yu, and Y. Gao, "Micro-cracks on electro-discharge machined surface and the fatigue failure of a diesel engine injector," *Engineering Failure Analysis*, vol. 13, pp. 124-133, 2013.
- [16] S. M. Bošnjaka, M. A. Arsićb, N. B. Gnjatovića, ILJ. Milenovića, and D. M. Arsićc, "Failure of the bucket wheel excavator buckets," *Engineering Failure Analysis*, vol. 84, pp. 247-261, 2018.
- [17] M. A. Khattaka, S. Zamana, S. Kazic, H. Ahmed, H. M. Habibe, H. M. Alie, and M. N. Tamina, "Failure investigation of welded 430 stainless steel plates for conveyor belts," *Engineering Failure Analysis*, vol. 116, 2020.
- [18] R. Guo, S. Xue, L. Zheng, A. Deng, and Lv. Liu, "Fracture failure analysis of DY08 Aluminum alloy elastic coupling," *Engineering Failure Analysis*, vol. 104, pp. 1030-1039, 2019.
- [19] H. R. Majidia, A.R. Torabib, M. Zabihia, S. M. J. Razavic, and F. Bertoc, "Energy-based ductile failure predictions in cracked friction-stir welded joints," *Engineering Failure Analysis*, vol. 102, pp. 327-337, 2019.
- [20] P. Moczko, D. Pietrusiak, and J. Wieckowski, "Investigation of the failure of the bucket wheel excavator bridge conveyor," *Engineering Failure Analysis*, vol. 106, 2019.
- [21] J. S. Rodrígueza, J. F. Duranb, Y. Aguilara, G. A. P. Alcázarb, and O. A. Zambranoa, "Failure analysis in sugar cane cutter base blades," *Engineering Failure Analysis*, vol. 112, 2020.
- [22] G. Vukelica, D. Pastorcicb, G. Vizentina, and Z. Bozic, "Failure investigation of a crane gear damage," *Engineering Failure Analysis*, vol. 115, 2020.
- [23] Q. Xiaofenga, L. Jie, Z. Xingguod, F. Lia, and P. Ruiqiang, "Fracture failure analysis of transmission gear shaft in a bidirectional gear pump," *Engineering Failure Analysis*, vol. 118, 2020.
- [24] R. Rajasekaran, A. K. Lakshminarayanan, R. Damodaram, and V. Balasubramanian, "Stress corrosion cracking failure of friction stir welded nuclear grade austenitic stainless steel," *Engineering Failure Analysis*, vol. 120, 2021.